

RISE: Rank in Similarity Graph Edge-Count Two-Sample Test

Doudou Zhou and Hao Chen

Department of Statistics, University of California, Davis

Abstract: Two-sample hypothesis testing for high-dimensional data is ubiquitous nowadays. Rank-based tests are popular nonparametric methods for univariate data. However, they are difficult to extend to high-dimensional data. In this paper, we propose a new family of non-parametric two-sample testing procedure, **Rank In Similarity graph Edge-count two-sample test (RISE)**. The new test statistic is constructed on a rank-weighted similarity graph, such as the k -nearest neighbor graph. As a result, RISE can also be applied to non-Euclidean data. Theoretically, we prove that, under some mild conditions, the new test statistic converges to the χ_2^2 distribution under the permutation null distribution, enabling a fast type-I error control. RISE exhibits good power under a wide range of alternatives compared to existing methods, as shown in extensive simulations. The new test is illustrated on the New York City taxi data for comparing travel patterns in consecutive months and a brain network dataset in comparing male and female subjects.

Keywords and phrases: Non-parametric two-sample test, rank-based method, similarity graph, high-dimensional data, non-Euclidean data.

1. Introduction

For two independent random samples $X_1, \dots, X_m \stackrel{i.i.d}{\sim} F_X$ and $Y_1, \dots, Y_n \stackrel{i.i.d}{\sim} F_Y$, we consider the test

$$H_0 : F_X = F_Y \text{ against } H_1 : F_X \neq F_Y .$$

Nowadays, it is common that the data is high-dimensional or non-Euclidean (Bullmore and Sporns, 2012; Tian et al., 2016; Menafoglio and Secchi, 2017; Jiang et al., 2020). In many of these problems, one has little information on F_X and F_Y , which makes parametric approaches not applicable when the dimension is high. A number of nonparametric tests have been proposed for high-dimensional data such as the graph-based tests (Friedman and Rafsky, 1979; Schilling, 1986; Henze, 1988; Rosenbaum, 2005; Chen and Zhang, 2013; Chen and Friedman, 2017; Chen, Chen and Su, 2018; Zhang and Chen, 2020), the classification-based tests (Hediger, Michel and Näf, 2019; Lopez-Paz and Oquab, 2016; Kim et al., 2021), the interpoint distances-based tests (Székely and Rizzo, 2013; Biswas and Ghosh, 2014; Li, 2018), and the kernel-based tests (Gretton et al., 2008; Harchaoui, Bach and Moulines, 2007; Gretton et al., 2009, 2012a; Song and Chen, 2020).

For non-parametric testing, rank-based tests are popular to approach given the success of the Wilcoxon's rank-sum test (Wilcoxon, 1945) for univariate

data. However, the rank for multivariate data is hard to define. There are some extended definitions of the rank to accommodate multivariate data, such as the spatial rank (Chaudhuri, 1996; Marden, 1999), the Mahalanobis rank (Hallin and Paindaveine, 2004, 2006), and the component-wise rank (Bickel, 1965; Puri and Sen, 2013). For instance, Oja (2010) proposed the multivariate spatial signs and ranks, which can be applied to construct a multivariate affine-invariant family of rank tests for the detection of the location difference. Based on the data depth rank, Liu and Singh (1993) proposed tests as a multivariate analog of Wilcoxon’s rank-sum test, and Barale and Shirke (2021) proposed a test that worked both for location and scale difference. However, these tests are mainly for low-dimensional data.

Recently, Pan et al. (2018) introduced Ball Divergence (BD) to measure the difference between two distributions and proposed a metric rank test procedure. Deb and Sen (2021) proposed to define the multivariate ranks through the theory of measure transportation (Hallin et al., 2021), based on which they built the multivariate rank-based distribution-free nonparametric testing. Both tests can be applied to high-dimensional data and achieved good performance for some useful settings. However, they also lose power under some common alternatives, which will be detailed in Section 4. Besides, they did not provide any analytic p -value approximations and relied on random permutations to obtain their p -values.

To address the problems, we propose a new framework of two-sample testing procedure, **R**ank **I**n **S**imilarity graph **E**dge-**C**ount two-sample test (RISE), which overcomes the curse of dimensionality (Chen and Friedman, 2017) and enables a fast type-I error control. Instead of dealing with the ranks of observations, we consider ranks on the similarity graph of the observations, such as the k -nearest neighbor (k -NN) graph (Henze, 1988) and the k -minimum spanning tree (k -MST)¹ graph (Friedman and Rafsky, 1979), which can be built from the pairwise distance of observations. As a result, our framework is applicable to non-Euclidean data as well.

Test statistics based on similarity graphs have attracted a lot of attention recently, as they can be applied to data with an arbitrary dimension and non-Euclidean data, and perform well for many high-dimensional settings. The first test of this type was proposed in Friedman and Rafsky (1979) using the k -MST graph, later Schilling (1986) and Henze (1988) used the k -NN graph, and Rosenbaum (2005) proposed to use the minimum distance non-bipartite pairing² (MDP) graph to obtain an exact distribution-free test, which was extended to k -MDP in Chen and Friedman (2017). Recently, Chen and Friedman (2017) proposed a new test statistic, the generalized edge-count test (GET), on simi-

¹The MST is a spanning tree connecting all observations while minimizing the sum of distances of edges in the tree. The k -MST is the union of the 1st, \dots , k th MSTs, where the k th MST is a spanning tree that connects all observations while minimizing the sum of distances across edges excluding edges in the $(k-1)$ -MST.

²The MDP is constructed by dividing the N observations into $N/2$ (assuming N is even) non-overlapping pairs while minimizing the $N/2$ distances within pairs. The k -MDP is the union of the 1st, \dots , k th MDPs, where the k th MDP is a minimum distance non-bipartite pairing while minimizing the sum of distances within pairs excluding pairs in the $(k-1)$ -MDP.

larity graphs that utilizes a common pattern for high-dimensional data, and the test works well for a variety of alternatives.

The current graph-based tests treat each edge in the graph equally and ignore the differences on edges (Friedman and Rafsky, 1979; Henze, 1988; Chen and Friedman, 2017), which could loss power. There were attempts to use ranks in earlier studies (Schilling, 1986; Rosenbaum, 2005), but these tests lack power for high-dimensional data under some common alternatives. RISE solves the problems by incorporating weights on the edges of the similarity graphs and proposing a Mahalanobis-type statistic that works well for a variety of settings where existing methods work poorly.

The rest of the paper is organized as follows. In Section 2, we introduce in detail the new test statistic T_R with its moment properties. The asymptotic property of T_R is presented in Section 3. Extensive simulations are conducted in Section 4 with real data applications presented in Section 5. The details of proofs of the theorems are deferred to Appendices and the Supplementary Materials.

2. A new test statistic

To simplify the notations, let

$$Z_i = X_i, i = 1, \dots, m; \quad Z_{m+j} = Y_j, j = 1, \dots, n$$

be the pooled samples and $N = m + n$. For a matrix $\mathbf{D} \in \mathbb{R}^{N \times N}$, we use D_{ij} to denote its (i, j) entry. Our test statistic is built from a rank matrix on the similarity graph obtained in the following steps.

Step I: Similarity matrix. Determine the similarity matrix $\mathbf{S} = (S_{ij})_{i,j=1}^N \in \mathbb{R}^{N \times N}$, where the larger the S_{ij} , the more similar the observations Z_i and Z_j are. For instance, the Euclidean distance can be used for the Euclidean data and \mathbf{S} can be defined as $S_{ij} = -\|Z_i - Z_j\|, i, j = 1, \dots, N$, where $\|\cdot\|$ is the Euclidean norm. For other choices of the distances, see Chen and Zhang (2013); Sarkar and Ghosh (2018); Sarkar, Biswas and Ghosh (2020).

Step II: Rank on the similarity graph. We first construct a similarity graph using the similarity matrix obtained in Step I. We require the similarity graph to have no self-loop. Some common choices of similarity graphs are the k -NN graph, k -MST graph and the k -MDP graph. We then construct the rank matrix $\mathbf{R} \in \mathbb{R}^{N \times N}$ on the similarity graph constructed by \mathbf{S} . Two types of rank are considered: the graph-based rank and the overall rank. To be specific, the graph-based rank is assigned in a descending order such that the value $k - j + 1$ is assigned to the edges in the j th subgraph (e.g., the j th NN graph or the j th MST) for $j = 1, \dots, k$. The overall rank is assigned by the rank of the similarities of the edges from \mathbf{S} such that $M - j + 1$ is assigned to the j th largest similarity of the edges for $j = 1, \dots, M$ where M is the number of edges in the similarity graph. We set $R_{ij} = 0$ if edge (i, j) is not in the similarity graph.

Remark 2.1. In the main context, we focus on the graph-based rank on the k -NN graph and the overall rank on the k -MDP graph as they are on the two ends

of the spectrum. The k -MST graph is very similar to that of the k -NN graph due to the internal link between the two types of graphs. Thus, we defer the assessment of the graph-based rank and the overall rank on the k -MST graph to Supplement S2. Our test statistic is not well-defined for the graph-based rank on the k -MDP, which will be shown in Theorem 2.2.

Besides the above mentioned similarity graphs, there are other choices of the similarity graphs such as the shared nearest neighbor graph (Ertoz, Steinbach and Kumar, 2002) and the shortest Hamiltonian path graph (Biswas, Mukhopadhyay and Ghosh, 2014), and the rank matrix can be defined in a similar way.

Remark 2.2. Instead of rank, other choices of weights can also be considered. For instance, the interpoint distance or the kernel values. By incorporating different weights, the performance of the test can be different. In this work, we focus on exploring using ranks.

Step III: Test statistic. We first define two basic quantities

$$U_x = \sum_{i=1}^m \sum_{j=1}^m R_{ij} \quad \text{and} \quad U_y = \sum_{i=m+1}^N \sum_{j=m+1}^N R_{ij}.$$

The proposed test statistic is defined as

$$T_R = (U_x - \mu_x, U_y - \mu_y) \boldsymbol{\Sigma}^{-1} \begin{pmatrix} U_x - \mu_x \\ U_y - \mu_y \end{pmatrix},$$

where $\mu_x = \mathbf{E}_P(U_x)$, $\mu_y = \mathbf{E}_P(U_y)$ and $\boldsymbol{\Sigma} = \mathbf{Cov}_P((U_x, U_y)^\top)$. We use \mathbf{P}_P , \mathbf{E}_P , \mathbf{Var}_P , \mathbf{Cov}_P to denote the probability, expectation, variance, and covariance under the permutation null distribution, respectively, which places $1/\binom{N}{m}$ probability on each of the $\binom{N}{m}$ permutations of the group labels where the first group has m observations and the second group has n observations.

Remark 2.3. The new test statistic T_R is similar to GET in terms of its formula while GET treats each edge in the similarity graph equally. Actually, when the weights on the similarity graph are all set to be one, T_R becomes GET when the similarity graph is undirected, and becomes the directed version of GET (Chu and Chen, 2018; Liu and Chen, 2020) when the similarity graph is directed. For GET, Chen and Friedman (2017) discussed that under the alternative hypothesis, there are two possible scenarios that (i) both samples tend to connect with each other within samples and (ii) one sample tends to connect within sample while the other sample tends to connect between sample. Similarly, for our rank quantities, under the alternative hypothesis, we also have two possible scenarios that (i) both U_x and U_y tend to be large and (ii) one of them tends to be large while the other one tends to be small. Hence, T_R can capture the two different type of scenarios and is powerful for a wider range of alternatives.

2.1. Moment properties

We first symmetrize \mathbf{R} by using $\frac{1}{2}(\mathbf{R} + \mathbf{R}^\top)$. With a slight notation abuse, in the following, \mathbf{R} is used for the symmetrised version. This does not change the values of U_x and U_y by their definitions; while the computation would be much simpler. Let $g_i = 1$ if the i th sample is from F_X and $g_i = 0$ if from F_Y . Then U_x and U_y can be rewritten as

$$U_x = \sum_{i=1}^N \sum_{j=1}^N g_i g_j R_{ij} \quad \text{and} \quad U_y = \sum_{i=1}^N \sum_{j=1}^N (1 - g_i)(1 - g_j) R_{ij}. \quad (1)$$

To simplify the notations, we further denote

$$\begin{aligned} R_{i\cdot} &= \sum_{j=1}^N R_{ij}, \quad \bar{R}_{i\cdot} = \frac{R_{i\cdot}}{N-1}, \quad r_0 = \frac{1}{N(N-1)} \sum_{i=1}^N \sum_{j=1}^N R_{ij}, \\ r_1^2 &= \frac{1}{N} \sum_{i=1}^N \bar{R}_{i\cdot}^2, \quad \text{and} \quad r_d^2 = \frac{1}{N(N-1)} \sum_{i=1}^N \sum_{j=1}^N R_{ij}^2. \end{aligned}$$

Theorem 2.1. *Under the permutation null distribution, we have*

$$\begin{aligned} \mathbf{E}_P(U_x) &= m(m-1)r_0, \quad \mathbf{E}_P(U_y) = n(n-1)r_0 \\ \mathbf{Var}_P(U_x) &= \frac{2mn(m-1)}{(N-2)(N-3)} ((n-1)(r_d^2 - r_0^2) + 2(m-2)(N-1)(r_1^2 - r_0^2)), \\ \mathbf{Var}_P(U_y) &= \frac{2mn(n-1)}{(N-2)(N-3)} ((m-1)(r_d^2 - r_0^2) + 2(n-2)(N-1)(r_1^2 - r_0^2)), \\ \mathbf{Cov}_P(U_x, U_y) &= \frac{2m(m-1)n(n-1)}{(N-2)(N-3)} ((r_d^2 - r_0^2) - 2(N-1)(r_1^2 - r_0^2)). \end{aligned}$$

The proof of Theorem 2.1 is in Appendix A. To assure that T_R is well-defined, the covariance matrix Σ should be invertible. Here we present the sufficient and necessary conditions.

Theorem 2.2. *Given $m, n \geq 2$, T_R is well-defined unless one of the following two cases happens:*

- (C1). $r_1^2 = r_0^2$;
- (C2). $(N-2)(r_d^2 - r_0^2) = 2(N-1)(r_1^2 - r_0^2)$.

The proof of Theorem 2.2 is in Appendix B. In the following, we briefly discuss the two cases. By definition,

$$r_0 = \frac{1}{N(N-1)} \sum_{i=1}^N \sum_{j=1}^N R_{ij} = \frac{1}{N} \sum_{i=1}^N \bar{R}_{i\cdot}.$$

is the average of both $\{R_{ij}\}_{i,j=1}^N$ and $\{\bar{R}_i\}_{i=1}^N$, so $r_d^2 - r_0^2$ is the variance of $\{R_{ij}\}_{i,j=1}^N$ and $r_1^2 - r_0^2$ is the variance of $\{\bar{R}_i\}_{i=1}^N$. For instance, the graph-based rank matrix on the k -MDP satisfies (C1) as all nodes are required to have the exact same degree k for the k -MDP graph and thus $\bar{R}_i = \frac{(1+k)k}{2(N-1)}$ for all i . Except for such special defined graph, it is rare to have graphs that satisfy (C1) or (C2). We check this through some simple simulations. We generate datasets from the standard multivariate Gaussian distribution with different N 's and d 's. For each dataset, we calculate the two ratios $\frac{r_1^2}{r_0^2}$ and $\frac{(N-2)(r_d^2 - r_0^2)}{2(N-1)(r_1^2 - r_0^2)}$. The procedure is repeated 1,000 times for each combination of $N \in \{50, 100, 200\}$ and $d \in \{50, 1000\}$ using \mathbf{R} constructed by the graph-based rank on the k -NN graph and the overall rank on the k -MDP graph, respectively, where k is set as 5, $\lceil \sqrt{N} \rceil$ and $\lceil N^{0.8} \rceil$, respectively. Here $\lceil \cdot \rceil$ rounds a real number to its nearest integer number. The boxplots are in Supplement S2. We find the two ratios are larger than one in all of these simulation runs. In practice, when we apply the method, we could easily check whether the two cases happen. If it unfortunately happens, which is rare, we could always use a different type of similarity graph to avoid the problem.

Define $U_w = \frac{n-1}{N-2}U_x + \frac{m-1}{N-2}U_y$ and $U_{\text{diff}} = U_x - U_y$, and their standardized statistics

$$Z_w^P = \frac{U_w - \mathbf{E}_P(U_w)}{\sigma_w^P}, \text{ and } Z_{\text{diff}}^P = \frac{U_{\text{diff}} - \mathbf{E}_P(U_{\text{diff}})}{\sigma_{\text{diff}}^P},$$

where $\sigma_w^P = \sqrt{\mathbf{Var}_P(U_w)}$ and $\sigma_{\text{diff}}^P = \sqrt{\mathbf{Var}_P(U_{\text{diff}})}$.

Theorem 2.3. *When T_R is well-defined, we have*

$$T_R = (Z_w^P)^2 + (Z_{\text{diff}}^P)^2, \quad (2)$$

and

$$\mathbf{Cov}_P(Z_w^P, Z_{\text{diff}}^P) = 0.$$

The proof of Theorem 2.3 is in Appendix C. By Theorem 2.1, it is easy to show that

$$(\sigma_w^P)^2 = \frac{2m(m-1)n(n-1)}{(N-2)^2(N-3)} \{(N-2)(r_d^2 - r_0^2) - 2(N-1)(r_1^2 - r_0^2)\}$$

and

$$(\sigma_{\text{diff}}^P)^2 = 4(N-1)mn(r_1^2 - r_0^2).$$

Based on the variance of U_w and U_{diff} , it is easy to see that when (C1) or (C2) happens, Z_{diff}^P or Z_w^P degenerates, respectively.

Remark 2.4. Some test statistics other than T_R can also be considered. For instance, the weighted rank sum statistic Z_w^P corresponding to the weighted

edge-count test (Chen, Chen and Su, 2018) that should work well for the location alternative and unbalanced sample sizes, and the max-rank test statistics $R_{\max} \equiv \max\{Z_w^P, |Z_{\text{diff}}^P|\}$ that corresponds to the max-type edge-count test statistic (Chu and Chen, 2019), which is preferred under the change-point setting.

3. Asymptotic properties

Obtaining the exact p -value of T_R by examining all permutations could be feasible for small sample sizes, but is time-prohibitive when the sample size is large. We thus work on the asymptotic distribution of T_R .

Before stating the theorem, we define some notations. Let $\xrightarrow{\mathcal{D}}$ be convergence in distribution, $a_n = o(b_n)$ be that a_n is dominated by b_n asymptotically, i.e., $\lim_{n \rightarrow \infty} \frac{a_n}{b_n} = 0$, $a_n = O(b_n)$ or $a_n \asymp b_n$ be that a_n is bounded both above and below by b_n asymptotically, $a_n \lesssim b_n$ be that a_n is bounded above by b_n (up to a constant factor) asymptotically, and ‘the usual limit regime’ be that $m, n \rightarrow \infty$ and $\frac{m}{n}$ does not go to 0 or ∞ asymptotically. The following is a list of sufficient conditions for deriving the asymptotic distribution of T_R .

$$\text{Condition 3.1. } \sum_{i=1}^N \left(\sum_{j=1}^N R_{ij}^2 \right)^2 \lesssim N^3 r_d^4.$$

$$\text{Condition 3.2. } \sum_{i=1}^N |\bar{R}_i - r_0|^3 = o\left((N(r_1^2 - r_0^2))^{\frac{3}{2}} \right).$$

$$\text{Condition 3.3. } \sum_{i=1}^N (\bar{R}_i - r_0)^3 = o(N r_d (r_1^2 - r_0^2)).$$

$$\text{Condition 3.4. } \left| \sum_{i \neq j \neq k}^N R_{ji} R_{ik} (\bar{R}_j - r_0) (\bar{R}_k - r_0) \right| = o(N^3 r_d^2 (r_1^2 - r_0^2)).$$

$$\text{Condition 3.5. } \sum_{i=1}^N \sum_{j=1}^N \sum_{k \neq i, j}^N \sum_{l \neq i, j}^N R_{ij} R_{kl} (R_{ik} R_{jl} + R_{il} R_{jk}) = o(N^4 r_d^4).$$

$$\text{Condition 3.6. } r_1 = o(r_d).$$

$$\text{Condition 3.7. } \max_{i, j} R_{ij} = o(N^2 r_d^2).$$

Theorem 3.1. *Let $\mathbf{R} = (R_{ij})_{i, j \in [N]}^{j \in [N]} \in \mathbb{R}^{N \times N}$ be a symmetric matrix with non-negative entries and zero diagonal elements. Suppose further $R_{ij} \geq 1$ if $R_{ij} > 0$. In the usual limit regime, under Conditions 3.1-3.7, we have that*

$$(Z_w^P, Z_{\text{diff}}^P)^\top \xrightarrow{\mathcal{D}} N_2(\mathbf{0}_2, \mathbf{I}_2) \quad \text{and} \quad T_R \xrightarrow{\mathcal{D}} \chi_2^2$$

under the permutation null distribution.

Remark 3.1. It should be noticed that Theorem 3.1 holds for any matrix \mathbf{R} satisfying the conditions, rather than just the rank matrices constructed in Section 2. As a result, we can use different ways to weight the similarity graph. Moreover, the matrix \mathbf{R} does not have to come from a similarity graph. For the condition $R_{ij} \geq 1$ if $R_{ij} > 0$, it could be easily extended to work for $R_{ij} \geq \delta$ if $R_{ij} > 0$ for any positive constant δ . When $\delta < 1$, the conditions would be modified by replacing R_{ij} with $\frac{R_{ij}}{\delta}$.

The proof of Theorem 3.1 is in Appendix D. For the conditions, Condition 3.7 holds trivially for the two types of rank matrices defined in Section 2. For Conditions 3.1-3.6, when R_{ij} 's only take values on 0 or 1 and $R_{ij} = 1$ if and only if the edge (i, j) is in the similarity graph, then Conditions 3.1-3.5 degenerate to the conditions in Zhu and Chen (2021) and Condition 3.6 holds trivially by plugging in R_{ij} 's. The following remark discuss further on Conditions 3.1-3.6.

Remark 3.2. Although Conditions 3.1-3.6 seem complex, following the proof in Zhu and Chen (2021), we can have another version of conditions that are a bit stronger but easier to understand. Assume G is a similarity graph from Step II:

$$G \equiv (V = \mathcal{N}, E = \{(i, j) : R_{ij} > 0, i, j \in \mathcal{N}\}),$$

where $\mathcal{N} = \{1, \dots, N\}$. Let G_i be the set of edges with one endpoint node i , $G_{i,2}$ be the set of edges with at least one endpoint in G_i . In addition, we use $|\cdot|$ to denote the cardinality of a set. So $|G|$ is the number edges in G . Let $V_G = \sum_{i=1}^N |G_i|^2 - 4|G|^2/N$ which describes the variability of the sequence $|G_i|$'s, and $V_R = \sum_{i=1}^N R_i^2 - (N(N-1)r_0)^2/N$. Then, Conditions 3.8-3.11 are sufficient conditions for obtaining the asymptotic distribution of T_R .

$$\text{Condition 3.8. } \sum_{i=1}^N |G_i|^2 = o(|G|^{\frac{3}{2}}).$$

$$\text{Condition 3.9. } \sum_{i=1}^N |G_{i,2}|^2 = o(|G|V_G).$$

$$\text{Condition 3.10. } \sum_{i=1}^N |G_i|^3 = o(\sqrt{|G| \wedge \overline{V_G V_G}}).$$

$$\text{Condition 3.11. } \sum_{i=1}^N \sum_{j=1}^N R_{ij}^2 \asymp K^2 |G|; \sum_{i=1}^N R_i^2 \asymp K^2 \sum_{i=1}^N |G_i|^2; V_R \asymp K^2 V_G, \text{ where } K = \max_{i,j \in [N]} R_{ij}.$$

This set of conditions tries to decouple the conditions on the graphs. Conditions 3.8-3.10 are borrowed from Zhu and Chen (2021), which are used to construct the limiting distributions of graph-based test statistics and shown to be satisfied easily by numerical experiments. Since we incorporate the weight (rank) information in the edges, we need an extra Condition 3.11, which is not hard to satisfy. For example, when \mathbf{R} is the graph-based rank on the k -NN graph, we have $K \asymp k$ and $\sum_{i=1}^N \sum_{j=1}^N R_{ij}^2 \geq N \sum_{l=1}^k (l/2)^2 = Nk(k+1)(2k+1)/24 \asymp K^2 |G|$ and $\sum_{i=1}^N \sum_{j=1}^N R_{ij}^2 \leq k^2 |G|$, which implies $\sum_{i=1}^N \sum_{j=1}^N R_{ij}^2 \asymp K^2 |G|$. We also know that $R_i^2 \geq (\sum_{l=1}^k l/2)^2 = k^2(k+1)^2/16$ and $R_i^2 \leq (k|G_i|)^2 = k^2 |G_i|^2$. If $|G_i| \asymp k$, we would have $\sum_{i=1}^N R_i^2 \asymp K^2 \sum_{i=1}^N |G_i|^2$.

4. Simulation studies

In this section, we conduct extensive simulations to examine the newly proposed test RISE. Specifically, we consider a wide range of null and alternative distributions in moderate/high dimensions, including multivariate Gaussian distribution, Gaussian mixture distribution, multivariate log-normal distribution and multivariate t_5 distribution. These different distributions range from light-tails to heavy-tails, and the alternatives range from location difference, scale

difference to mixed alternatives, with a hope that these simulation settings can cover real world scenarios.

We compare the type-I error and statistical power with seven state-of-art methods, including two graph-based methods: GET on k -MST using the R package *gTests* (Chen and Friedman, 2017), Rosenbaum’s cross matching test (CM) using the R package *crossmatch* (Rosenbaum, 2005); two rank-based methods: multivariate rank-based test using measure transportation (MT) (Deb and Sen, 2021) and non-parametric two-sample test based on ball divergence (BD) using the R package *Ball* (Pan et al., 2018); and three other tests: an LP-nonparametric test statistic (GLP) using the R package *LPKsample* (Mukhopadhyay and Wang, 2020), a high-dimensional low sample size k -sample tests (HD) using the R package *HDLSSkST* (Paul, De and Ghosh, 2021) and a kernel based two-sample test (MMD) using the R package *kerTests* (Gretton et al., 2012b). Finally, we denote our method as R_g -NN and R_o -MDP for RISE on the k -NN graph with the graph-based rank and on the k -MDP graph with the overall rank, respectively.

4.1. The Choice of k

For the tests based on similarity graphs, the choice of graph is an open question. Some previous works (Friedman and Rafsky, 1979; Zhang and Chen, 2020; Chen and Friedman, 2017; Chen, Chen and Su, 2018) suggested to use the k -MST and set k as a small constant number, e.g., $k = 3$ or $k = 5$. Recently, Zhu and Chen (2021) observed that a denser graph can improve the power of the tests such that $k = O(N^\lambda)$ for some $0 < \lambda < 1$ where N is the total number of observations. Following this, Zhang and Chen (2021) compared the power for different λ ’s under various simulation settings and suggested to use $\lambda = 0.5$ for GET, where it showed adequate power across different simulation settings. For RISE, we adopt a similar procedure. We generate i.i.d. samples of $X_i \sim F_X$ and $Y_i \sim F_Y$, and set $d = 500$ and vary the sample sizes (m, n) . Three combinations of (F_X, F_Y) are considered. Figure 1 shows how the power varies with λ such that $k = \lceil N^\lambda \rceil$ and the nominal significance level is set as 0.05. We see that the optimal k varies for different settings and it is reasonable to choose $\lambda = 0.65$ for both the k -NN and the k -MDP graphs to achieve adequate power. So in the following comparison of the simulation and real data analysis, we set $k = \lceil N^{0.5} \rceil$ for GET and $k = \lceil N^{0.65} \rceil$ for RISE on the k -NN and k -MDP graphs. In addition, we use their asymptotic distributions to obtain the p -values.

4.2. Settings

Throughout the simulation, we choose $m = n = 50$ and $m = 50, n = 100$, and set $d \in \{200, 500, 1000\}$. We consider diverse settings to examine the performance of these methods thoroughly. For each setting, we fix the distribution of \mathbf{X} as F_X , and choose different F_Y ’s for the alternative hypothesis. We set the parameters of the distributions to make the tests have moderate power to be comparable.

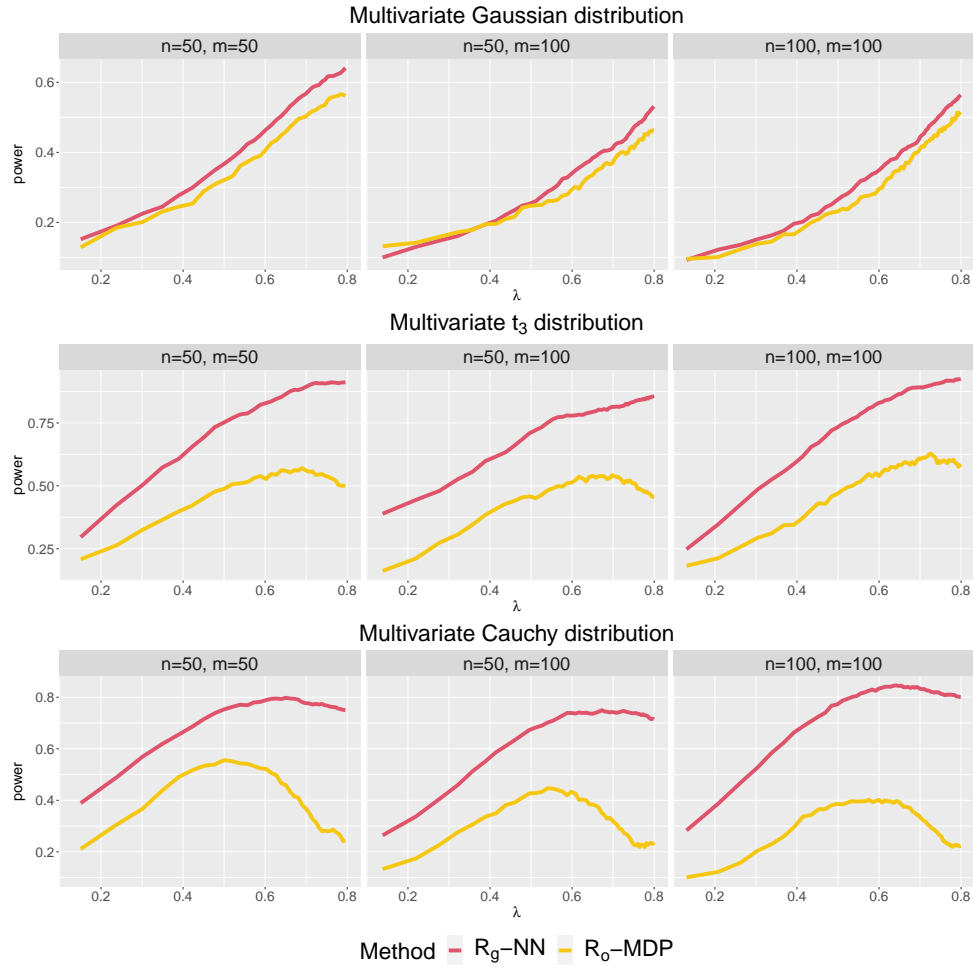


FIG 1. Estimated power of RISE on $[N^\lambda]$ -NN graph using the graph-based rank (R_g -NN) and $[N^\lambda]$ -MDP graph using the overall rank (R_o -MDP) over 1000 times of repetitions under each setting. The three settings are: $(N_d(\mathbf{0}_d, \mathbf{I}_d), N_d(\delta_1 \mathbf{1}_d, \mathbf{I}_d))$, $(t_3(\mathbf{0}_d, \mathbf{I}_d), t_3(\delta_2 \mathbf{1}_d, \delta_3 \mathbf{I}_d))$ and $(\text{Cauchy}_d(\mathbf{0}_d, \mathbf{I}_d), \text{Cauchy}_d(\delta_4 \mathbf{1}_d, \mathbf{I}_d))$ where $\delta_1 = \frac{20}{\sqrt{Nd}}$, $\delta_2 = \frac{28}{\sqrt{Nd}}$, $\delta_3 = (1 + \frac{25}{\sqrt{Nd}})^2$ and $\delta_4 = \frac{1.44}{\sqrt{Nd}}$. Here δ_i 's are set to make these tests have moderate power.

Each configuration is repeated 1000 times to estimate the power where the nominal significance level α is set as 0.05. Besides, we check the empirical sizes by setting $F_Y = F_X$ for $\alpha = 0.01$ and $\alpha = 0.05$ to check the asymptotic p -value approximation of RISE. The four settings are as follows:

- Setting I. $F_X = N_d(\mathbf{0}_d, \Sigma_X)$ is the multivariate Gaussian distribution, where $\Sigma_{X,ij} = .6^{|i-j|}$, $i, j \in [d]$.
- (a) Simple location: $F_Y = N_d(\delta \mathbf{1}_d, \Sigma_X)$ where $\delta = .5 \log d / \sqrt{d}$.
 - (b) Directed location: $F_Y = N_d(\boldsymbol{\mu}, \Sigma_X)$ where $\boldsymbol{\mu} = .5 \log d \boldsymbol{\mu}' / \|\boldsymbol{\mu}'\|_2$ and $\boldsymbol{\mu}' \sim N_d(\mathbf{0}_d, \mathbf{I}_d)$ is fixed.
 - (c) Simple scale: $F_Y = N_d(\mathbf{0}_d, \sigma^2 \Sigma_X)$ where $\sigma = 1 + .1 \log d / \sqrt{d}$.
 - (d) Correlated scale: $F_Y = N_d(\mathbf{0}_d, \Sigma_Y)$ where $\Sigma_{Y,ij} = .15^{|i-j|}$, $i, j \in [d]$.
 - (e) Location and scale mixed: $F_Y = N_d(\boldsymbol{\mu}, \Sigma_Y)$ where $\boldsymbol{\mu} = .2 \log d \boldsymbol{\mu}' / \|\boldsymbol{\mu}'\|_2$ and $\boldsymbol{\mu}' \sim N_d(\mathbf{0}_d, \mathbf{I}_d)$ is fixed.
- Setting II. $F_X = WN_d(.3\mathbf{1}_d, \mathbf{I}_d) + (1 - W)N_d(-.3\mathbf{1}_d, 2\mathbf{I}_d)$ is the Gaussian mixture distribution, where $W \sim \text{Bernoulli}(.5)$.
- (a) Location: $F_Y = WN_d((.3 + .75/\log d)\mathbf{1}_d, \mathbf{I}_d) + (1 - W)N_d(-(.3 + .75/\log d)\mathbf{1}_d, 2\mathbf{I}_d)$.
 - (b) Scale: $F_Y = WN_d(.3\mathbf{1}_d, (1 + \sigma)^2 \mathbf{I}_d) + (1 - W)N_d(-.3\mathbf{1}_d, (\sqrt{2} + \sigma)^2 \mathbf{I}_d)$, where $\sigma = .12\sqrt{50/d}$.
 - (c) Location and scale mixed: $F_Y = WN_d(.35\mathbf{1}_d, \Sigma_Y) + (1 - W)N_d(-.35\mathbf{1}_d, 2\Sigma_Y)$, where $\Sigma_{Y,ij} = .5^{|i-j|}$, $i, j \in [d]$.
- Setting III. $F_X = \exp(N_d(\mathbf{0}_d, \Sigma_X))$ is the multivariate log-normal distribution, where $\Sigma_{X,ij} = .6^{|i-j|}$, $i, j \in [d]$.
- (a) Simple location: $F_Y = \exp(N_d(\delta \mathbf{1}_d, \Sigma_X))$ where $\delta = .5 \log d / \sqrt{d}$.
 - (b) Sparse location: $F_Y = \exp(N_d(\boldsymbol{\mu}, \Sigma_X))$ where $\mu_j = (-1)^j 2.8 \log d / \sqrt{d}$, $j = 1, \dots, \lfloor .05d \rfloor$, $\mu_j = 0$, $j = \lfloor .05d \rfloor + 1, \dots, d$.
 - (c) Scale: $F_Y = \exp(N_d(\mathbf{0}_d, \Sigma_Y))$, where $\Sigma_{Y,ij} = .9(.1)^{|i-j|}$, $i, j \in [d]$.
 - (d) Location and scale mixed: $\mathbf{Y} = \exp(N_d(\delta \mathbf{1}_d, \sigma \Sigma_X))$ where $\sigma = 1 + .1(50/d)^{.25}$ and $\delta = .25 \log d / \sqrt{d}$.
- Setting IV. $F_X = t_5(\mathbf{0}_d, \Sigma_X)$ is the multivariate t_5 distribution, where $\Sigma_{X,ij} = .6^{|i-j|}$, $i, j \in [d]$.
- (a) Simple location: $F_Y = t_5(\delta \mathbf{1}_d, \Sigma_X)$ where $\delta = .5 \log d / \sqrt{d}$.
 - (b) Sparse location: $F_Y = t_5(\boldsymbol{\mu}, \Sigma_X)$ where $\mu_j = (-1)^j 2.1 \log d / \sqrt{d}$, $j = 1, \dots, \lfloor .05d \rfloor$, $\mu_j = 0$, $j = \lfloor .05d \rfloor + 1, \dots, d$.
 - (c) Scale: $F_Y = t_5(\mathbf{0}_d, \Sigma_Y)$, where $\Sigma_{Y,ij} = .7(.1)^{|i-j|}$, $i, j \in [d]$.
 - (d) Location and scale mixed: $\mathbf{Y} = t_5(\delta \mathbf{1}_d, \Sigma_Y)$ where $\Sigma_{Y,ij} = (.8)^{|i-j|}$, $i, j \in [d]$ and $\delta = .5 \log d / \sqrt{d}$.

TABLE 1
 Empirical sizes of the tests under the four settings when the nominal significance level $\alpha = .01$ and 0.05, respectively, for $m = n = 50$ and $d = 200, 500, 1000$.

| $\alpha = 0.01$ Method | Setting I | | | Setting II | | | Setting III | | | Setting IV | | |
|---------------------------|-----------|------|------|------------|------|------|-------------|------|------|------------|------|------|
| | 200 | 500 | 1000 | 200 | 500 | 1000 | 200 | 500 | 1000 | 200 | 500 | 1000 |
| R _g -NN | 0.01 | 0.01 | 0.01 | 0.01 | 0.01 | 0.01 | 0.01 | 0.01 | 0.00 | 0.01 | 0.01 | 0.01 |
| R _o -MDP | 0.01 | 0.01 | 0.01 | 0.02 | 0.03 | 0.02 | 0.02 | 0.02 | 0.01 | 0.01 | 0.01 | 0.02 |
| GET | 0.01 | 0.01 | 0.01 | 0.01 | 0.01 | 0.00 | 0.01 | 0.01 | 0.01 | 0.02 | 0.01 | 0.01 |
| CM | 0.01 | 0.01 | 0.00 | 0.01 | 0.01 | 0.01 | 0.01 | 0.01 | 0.01 | 0.01 | 0.00 | 0.01 |
| MT | 0.01 | 0.01 | 0.02 | 0.01 | 0.01 | 0.00 | 0.01 | 0.01 | 0.01 | 0.01 | 0.01 | 0.01 |
| BD | 0.01 | 0.01 | 0.01 | 0.01 | 0.01 | 0.01 | 0.01 | 0.01 | 0.00 | 0.01 | 0.01 | 0.01 |
| GLP | 0.01 | 0.01 | 0.01 | 0.02 | 0.03 | 0.03 | 0.06 | 0.07 | 0.06 | 0.01 | 0.01 | 0.01 |
| HD | 0.00 | 0.01 | 0.00 | 0.00 | 0.01 | 0.00 | 0.00 | 0.01 | 0.00 | 0.00 | 0.00 | 0.00 |
| MMD | 0.00 | 0.00 | 0.00 | 0.00 | 0.00 | 0.00 | 0.00 | 0.00 | 0.00 | 0.00 | 0.00 | 0.00 |
| $\alpha = 0.05$ Method | Setting I | | | Setting II | | | Setting III | | | Setting IV | | |
| | 200 | 500 | 1000 | 200 | 500 | 1000 | 200 | 500 | 1000 | 200 | 500 | 1000 |
| R _g -NN | 0.05 | 0.06 | 0.04 | 0.05 | 0.04 | 0.05 | 0.05 | 0.04 | 0.04 | 0.06 | 0.05 | 0.06 |
| R _o -MDP | 0.05 | 0.05 | 0.04 | 0.05 | 0.06 | 0.05 | 0.06 | 0.05 | 0.04 | 0.05 | 0.05 | 0.05 |
| GET | 0.04 | 0.05 | 0.04 | 0.04 | 0.06 | 0.04 | 0.04 | 0.05 | 0.04 | 0.06 | 0.06 | 0.06 |
| CM | 0.04 | 0.04 | 0.03 | 0.04 | 0.03 | 0.04 | 0.03 | 0.03 | 0.04 | 0.04 | 0.03 | 0.03 |
| MT | 0.05 | 0.05 | 0.06 | 0.04 | 0.05 | 0.05 | 0.05 | 0.06 | 0.07 | 0.05 | 0.05 | 0.04 |
| BD | 0.04 | 0.05 | 0.06 | 0.04 | 0.06 | 0.04 | 0.05 | 0.05 | 0.05 | 0.05 | 0.05 | 0.05 |
| GLP | 0.06 | 0.05 | 0.06 | 0.07 | 0.08 | 0.07 | 0.10 | 0.09 | 0.09 | 0.06 | 0.06 | 0.05 |
| HD | 0.03 | 0.04 | 0.03 | 0.03 | 0.04 | 0.03 | 0.02 | 0.03 | 0.02 | 0.02 | 0.02 | 0.02 |
| MMD | 0.00 | 0.00 | 0.00 | 0.00 | 0.01 | 0.00 | 0.01 | 0.00 | 0.00 | 0.01 | 0.00 | 0.01 |

4.3. Results

Here we present the results for $m = n = 50$ and $d \in \{200, 500, 1000\}$. The results for $m = 50, n = 100$ show similar patterns and are deferred to Supplement S2. Besides, a detailed comparison between RISE and GET including the results of RISE on the k -MST graph with the graph-based rank and the overall rank is provided in Supplement S2.

From Table 1, we see that RISE can control the type-I error well for different significant levels and settings, which validates the effectiveness of the asymptotic approximation even for relatively small sample sizes ($m = n = 50$). For other tests, MMD seems a little conservative and GLP has somewhat inflated type-I error for some settings, while all of the other tests can control the type-I error well.

The estimated power of the tests is presented in Tables 2-4. The highest power for each setting as well as those with power higher than 95% of the highest one are highlighted in bold type.

Table 2 shows the results for the multivariate Gaussian distribution and the Gaussian mixture distribution settings. From Table 2, we see that for the multivariate Gaussian distribution, under the simple location alternative (a), MT performs the best, followed immediately by R_g-NN and R_o-MDP. Under the directed location alternative (b), R_g-NN outperforms all of the other tests, followed immediately by R_o-MDP, then by GET. MMD is also good for $d = 200$, while all of other tests have low power. Under the simple scale alternative (c), BD and R_o-MDP perform the best and R_g-NN performs the second best. GET

TABLE 2

Estimated power of the tests with $\alpha = 0.05$ under the multivariate Gaussian distribution
 Setting I: (a) simple location, (b) directed location, (c) simple scale, (d) correlated scale,
 and (e) location and scale mixed and the Gaussian mixture distribution Setting II: (a)
 location, (b) scale, and (c) location and scale mixed for $m = n = 50$ and $d = 200, 500, 1000$.

| Method | Setting I (a) | | | Setting I (b) | | | Setting I (c) | | | Setting I (d) | | |
|---------------------|---------------|-------------|-------------|----------------|-------------|-------------|----------------|-------------|-------------|----------------|-------------|-------------|
| | 200 | 500 | 1000 | 200 | 500 | 1000 | 200 | 500 | 1000 | 200 | 500 | 1000 |
| R _g -NN | 0.85 | 0.82 | 0.80 | 0.98 | 0.93 | 0.88 | 0.88 | 0.96 | 0.98 | 0.79 | 0.77 | 0.76 |
| R _o -MDP | 0.80 | 0.78 | 0.74 | 0.96 | 0.89 | 0.81 | 0.93 | 0.98 | 0.99 | 0.73 | 0.75 | 0.76 |
| GET | 0.82 | 0.81 | 0.76 | 0.95 | 0.92 | 0.80 | 0.86 | 0.96 | 0.98 | 0.33 | 0.29 | 0.28 |
| CM | 0.30 | 0.27 | 0.22 | 0.38 | 0.29 | 0.24 | 0.04 | 0.04 | 0.05 | 0.63 | 0.63 | 0.63 |
| MT | 0.98 | 0.96 | 0.93 | 0.07 | 0.06 | 0.07 | 0.05 | 0.07 | 0.06 | 0.13 | 0.14 | 0.14 |
| BD | 0.79 | 0.61 | 0.41 | 0.52 | 0.37 | 0.23 | 0.96 | 0.99 | 1.00 | 0.15 | 0.16 | 0.14 |
| GLP | 0.55 | 0.49 | 0.22 | 0.15 | 0.15 | 0.08 | 0.09 | 0.05 | 0.06 | 0.07 | 0.06 | 0.06 |
| HD | 0.04 | 0.04 | 0.03 | 0.03 | 0.03 | 0.04 | 0.74 | 0.89 | 0.96 | 0.08 | 0.09 | 0.07 |
| MMD | 0.90 | 0.54 | 0.06 | 0.98 | 0.54 | 0.03 | 0.00 | 0.00 | 0.00 | 0.00 | 0.00 | 0.00 |
| Method | Setting I (e) | | | Setting II (a) | | | Setting II (b) | | | Setting II (c) | | |
| | 200 | 500 | 1000 | 200 | 500 | 1000 | 200 | 500 | 1000 | 200 | 500 | 1000 |
| R _g -NN | 0.94 | 0.90 | 0.90 | 0.56 | 0.72 | 0.87 | 0.55 | 0.54 | 0.56 | 0.50 | 0.41 | 0.39 |
| R _o -MDP | 0.91 | 0.89 | 0.89 | 0.49 | 0.56 | 0.67 | 0.20 | 0.23 | 0.24 | 0.17 | 0.15 | 0.15 |
| GET | 0.54 | 0.46 | 0.43 | 0.46 | 0.67 | 0.86 | 0.58 | 0.58 | 0.59 | 0.24 | 0.23 | 0.22 |
| CM | 0.71 | 0.69 | 0.71 | 0.14 | 0.20 | 0.23 | 0.04 | 0.04 | 0.04 | 0.53 | 0.55 | 0.57 |
| MT | 0.16 | 0.14 | 0.11 | 0.49 | 0.54 | 0.56 | 0.04 | 0.05 | 0.05 | 0.07 | 0.11 | 0.12 |
| BD | 0.20 | 0.19 | 0.18 | 0.37 | 0.47 | 0.63 | 0.39 | 0.29 | 0.30 | 0.06 | 0.09 | 0.11 |
| GLP | 0.09 | 0.09 | 0.05 | 0.08 | 0.08 | 0.07 | 0.09 | 0.08 | 0.08 | 0.08 | 0.08 | 0.08 |
| HD | 0.08 | 0.07 | 0.07 | 0.03 | 0.04 | 0.02 | 0.03 | 0.04 | 0.03 | 0.03 | 0.04 | 0.02 |
| MMD | 0.01 | 0.00 | 0.00 | 0.01 | 0.02 | 0.01 | 0.00 | 0.01 | 0.00 | 0.01 | 0.01 | 0.00 |

and HD also have satisfactory performance, while all of other tests have much lower power. Under the correlated scale alternative (d), R_g-NN and R_o-MDP exhibit the highest power and CM is also good enough. Under the location and scale mixed alternative (e), R_g-NN and R_o-MDP perform the best again, CM and GET have moderate power, and other tests such as MT and BD have low power. So basically, both R_g-NN and R_o-MDP perform well in the multivariate Gaussian distribution setting, across a wide range of alternatives, while other tests can perform well in some alternatives, but have low power in other alternatives. For the Gaussian mixture distribution setting II, we see that under the location alternative (a), R_g-NN performs the best. R_o-MDP, GET, MT and BD have moderate power while all of other tests have low power. Under the scale alternative (b), GET outperforms all of the other tests and R_g-NN also has satisfactory performance. Under the location and scale mixed alternative (c), CM performs the best and R_g-NN follows it. So the overall performance of R_g-NN is the best in the Gaussian mixture setting.

Table 3 shows the result of the multivariate log-normal distribution setting. We see that under the simple location alternative (a), MT performs the best when d is 200, and R_o-MDP performs the best when d is 500 and 1000. R_g-NN, GET, GLP and BD also perform well. Under the sparse location alternative (b), R_g-NN outperforms all of the other tests, followed by R_o-MDP and GET, especially when d is low ($d = 200$ or 500). MMD also performs well for $d = 200$ while other tests have low power. Under the scale alternative (c), R_o-MDP per-

TABLE 3

Estimated power of the tests with $\alpha = 0.05$ under the multivariate log-normal distribution
 Setting III: (a) simple location, (b) sparse location, (c) scale, and (d) location and scale
 mixed for $m = n = 50$ and $d = 200, 500, 1000$.

| Method | Setting III (a) | | | Setting III (b) | | | Setting III (c) | | | Setting III (d) | | |
|---------------------|-----------------|-------------|-------------|-----------------|-------------|-------------|-----------------|-------------|-------------|-----------------|-------------|-------------|
| | 200 | 500 | 1000 | 200 | 500 | 1000 | 200 | 500 | 1000 | 200 | 500 | 1000 |
| R _g -NN | 0.86 | 0.88 | 0.88 | 0.99 | 0.97 | 0.92 | 0.17 | 0.37 | 0.74 | 0.66 | 0.77 | 0.78 |
| R _o -MDP | 0.96 | 0.96 | 0.96 | 0.97 | 0.96 | 0.89 | 0.47 | 0.84 | 0.99 | 0.83 | 0.89 | 0.94 |
| GET | 0.80 | 0.81 | 0.83 | 0.95 | 0.88 | 0.66 | 0.14 | 0.32 | 0.70 | 0.64 | 0.76 | 0.79 |
| CM | 0.18 | 0.17 | 0.15 | 0.32 | 0.30 | 0.25 | 0.30 | 0.41 | 0.50 | 0.09 | 0.10 | 0.12 |
| MT | 0.97 | 0.94 | 0.88 | 0.11 | 0.25 | 0.43 | 0.20 | 0.28 | 0.30 | 0.68 | 0.65 | 0.60 |
| BD | 0.91 | 0.93 | 0.94 | 0.17 | 0.14 | 0.10 | 0.47 | 0.86 | 0.99 | 0.82 | 0.91 | 0.94 |
| GLP | 0.70 | 0.65 | 0.30 | 0.23 | 0.36 | 0.15 | 0.18 | 0.14 | 0.11 | 0.22 | 0.18 | 0.11 |
| HD | 0.29 | 0.36 | 0.43 | 0.04 | 0.04 | 0.04 | 0.23 | 0.46 | 0.65 | 0.24 | 0.34 | 0.44 |
| MMD | 0.83 | 0.57 | 0.20 | 0.98 | 0.79 | 0.08 | 0.12 | 0.10 | 0.06 | 0.54 | 0.32 | 0.10 |

TABLE 4

Estimated power of the tests with $\alpha = 0.05$ under the multivariate t_5 distribution Setting IV:
 (a) simple location, (b) sparse location, (c) scale and (d) location and scale mixed for
 $m = n = 50$ and $d = 200, 500, 1000$.

| Method | Setting IV (a) | | | Setting IV (b) | | | Setting IV (c) | | | Setting IV (d) | | |
|---------------------|----------------|-------------|-------------|----------------|-------------|-------------|----------------|-------------|-------------|----------------|-------------|-------------|
| | 200 | 500 | 1000 | 200 | 500 | 1000 | 200 | 500 | 1000 | 200 | 500 | 1000 |
| R _g -NN | 0.91 | 0.82 | 0.75 | 0.92 | 0.80 | 0.68 | 0.82 | 0.69 | 0.69 | 0.90 | 0.82 | 0.77 |
| R _o -MDP | 0.84 | 0.74 | 0.64 | 0.82 | 0.70 | 0.55 | 0.87 | 0.84 | 0.84 | 0.86 | 0.79 | 0.71 |
| GET | 0.69 | 0.48 | 0.26 | 0.58 | 0.36 | 0.20 | 0.60 | 0.46 | 0.50 | 0.73 | 0.55 | 0.34 |
| CM | 0.24 | 0.21 | 0.18 | 0.24 | 0.20 | 0.17 | 0.72 | 0.68 | 0.67 | 0.45 | 0.41 | 0.42 |
| MT | 0.95 | 0.92 | 0.88 | 0.10 | 0.09 | 0.06 | 0.17 | 0.19 | 0.19 | 0.75 | 0.72 | 0.67 |
| BD | 0.06 | 0.06 | 0.05 | 0.05 | 0.05 | 0.05 | 0.66 | 0.66 | 0.69 | 0.07 | 0.06 | 0.05 |
| GLP | 0.52 | 0.40 | 0.18 | 0.08 | 0.10 | 0.06 | 0.39 | 0.39 | 0.39 | 0.51 | 0.39 | 0.30 |
| HD | 0.02 | 0.02 | 0.02 | 0.03 | 0.02 | 0.02 | 0.13 | 0.11 | 0.11 | 0.02 | 0.03 | 0.01 |
| MMD | 0.62 | 0.17 | 0.04 | 0.42 | 0.09 | 0.03 | 0.30 | 0.29 | 0.35 | 0.60 | 0.20 | 0.05 |

forms the best, followed by BD. Under the mixed alternative, R_o-MDP performs the best, followed immediately by BD, R_g-NN, and GET. So the overall performance of R_o-MDP is the best under the multivariate log-normal distribution setting.

Finally, Table 4 shows the result of the multivariate t distribution. Both MT and R_g-NN perform well under the simple location alternative (a), and R_g-NN outperforms all of the other tests notably under the sparse location alternative (b). Both R_g-NN and R-MST perform well in the scale alternative (c) and R_g-NN performs the best in the mixed alternative (d). Basically, the overall performance of R_g-NN is the best under the multivariate t_5 distribution setting.

To summarize, we observe that MT performs well in the simple location alternative (Setting I (a), III (a), IV (a)) but lacks power in directed or sparse location alternative and scale alternatives, while BD performs well in the simple scale alternative but lacks power in the location alternatives. GET is doing a good job overall, but it is outperformed by RISE in most of the settings. Specifically, for settings GET loses power, RISE still performs well.

TABLE 5

The p -values of the tests showing inconsistent conclusion at 0.05 significance level for the NYC taxi data.

| Method | Jan vs Feb | Jul vs Aug | Aug vs Sep |
|---------------------|--------------|--------------|-------------|
| R _g -NN | 0.017 | 0.033 | 0.00 |
| R _o -MDP | 0.024 | 0.027 | 0.00 |
| GET | 0.231 | 0.072 | 0.00 |
| BD | 0.340 | 0.310 | 0.07 |

5. Real data analysis

5.1. New York City taxi data

To illustrate the proposed tests, we here conduct an analysis on whether the travel patterns are different in consecutive months in the New York City. We use New York City taxi data from the NYC Taxi Limousine Commission (TLC) website (<https://www1.nyc.gov/site/tlc/about/tlc-trip-record-data.page>). The data contains rich information such as the taxi pickup and drop-off date/times, longitude and latitude coordinates of pickup and drop-off locations. Specifically, we are interested in the travel pattern from the John F. Kennedy International Airport of the year 2015. Similarly to [Chu and Chen \(2019\)](#), we set the boundary of JFK airport from 40.63 to 40.66 latitude and from -73.80 to -73.77 longitude. Additionally, we set the boundary of New York City from 40.577 to 41.5 latitude and from -74.2 to -73.6 longitude. We only consider those trips that began with a pickup at JFK and ended with a drop-off in New York City. The New York City is then split into a 30×30 grid with equal size and the numbers of taxi drop-offs that fall within each cell are counted for each day. Thus each day is represented by a 30×30 matrix and we use the Frobenius norm to construct the similarity matrix \mathbf{S} .

We then conduct eleven comparisons over the consecutive months: January vs February, February vs March, \dots , November vs December. With the aim to illustrate the new tests, we treat them as eleven separate tests rather than a multiple testing problem. For simplicity, we only compare our method with GET and BD as the two tests perform well in the simulations compared to others. The four tests provide different conclusions for three comparisons at 0.05 significance level, which is presented in Table 5. The p -values of the eight comparisons with the same conclusion are presented in Table 6.

We notice that for these inconsistent conclusions, our methods always have p -values smaller than 0.05. Since both RISE and GET reject August vs September, and BD has the p -value close to 0.05, we take a closer look at the other two comparisons (Jan vs Feb, and Jul vs Aug) where the differences among the tests are more significant. The sample sizes are 59 and 62 for these two comparisons, respectively. Hence, 8-MST was used for GET. We next examine each k th MST and k -MST separately for $k = 1, \dots, 8$. Since the test statistic of GET depends on how far the two within-sample edge-counts deviate from their expectations under the null distribution, we check how the two edge-counts statistics change

TABLE 6
 The p -values of the tests showing consistent conclusion for the NYC taxi data.

| Method | Feb vs Mar | Mar vs Apr | Apr vs May | May vs Jun |
|------------|------------|------------|------------|------------|
| R_g -NN | 0.005 | 0.00 | 0.133 | 0.064 |
| R_o -MDP | 0.004 | 0.00 | 0.142 | 0.838 |
| GET | 0.010 | 0.00 | 0.754 | 0.343 |
| BD | 0.050 | 0.02 | 0.190 | 0.280 |
| Method | Jun vs Jul | Sep vs Oct | Oct vs Nov | Nov vs Dec |
| R_g -NN | 0.00 | 0.002 | 0.000 | 0.083 |
| R_o -MDP | 0.00 | 0.001 | 0.002 | 0.479 |
| GET | 0.00 | 0.001 | 0.000 | 0.108 |
| BD | 0.04 | 0.030 | 0.010 | 0.270 |

when k increases from 1 to 8. Table 7 shows the within-sample edge-counts of each sample in each k th MST. The p -values of GET on the k th MST and the k -MST for different k 's are also presented. For comparison, we also show the p -values of RISE on the k -MST graphs (denoted by R_g -MST). We notice that for most of the k th MSTs, at least one of the within-sample edge-counts somewhat deviates from their corresponding expectations. However, since GET treats all MSTs equally, there are two problems with it: (i) different MSTs can contain opposite information and (ii) a k th MST for a large k can contain noisier information. The first problem is obvious from the edge-counts statistics. For example, the sample February has the edge-counts above the expectation for the first to the fourth MSTs, but has the edge-count below the expectation for the fifth MST. This makes the p -value increases from 0.003 on the 4-MST to 0.09 on the 5-MST. Then again, the opposite trend of the edge-counts in sample February on the sixth MST to eighth MST makes the p -value increases persistently to the non-significant level finally. The second problem can be observed from the p -values of GET on the k th MST. The p -values of the two comparisons on the 1st MST are both small, but they can be very large for other k th MSTs. When the k th MST does not contain useful information but noise, the consequence for GET is much larger. On the other hand, RISE is less affected by the two problems by incorporating weights.

5.2. Brain network data

We here evaluate the performance of RISE in distinguishing differences in brain connectivity between male and female subjects using brain networks constructed from diffusion magnetic resonance imaging (dMRI). The data from the HNU1 study (Zuo et al., 2014) consists of dMRI records of fifteen male and fifteen female healthy subjects that were scanned ten times each over a period of one month. Processing the data by the same way as Arroyo et al. (2021), we constructed 300 weighted networks (one per subject and scan) with 200 nodes registered to the CC200 atlas (Craddock et al., 2012) using the NeuroData's MRI to Graphs pipeline (Kiar et al., 2018). Figure 2 plots four networks with two networks from male subjects and two from female subjects. The networks

TABLE 7

The edge-count statistics on the k th MST and the p -values of GET using the k th MST and the k -MST graph, and of RISE using the graph-based rank on the k -MST graph (R_g -MST), respectively. The expected edges for each MST are 15.763, 12.814, 15 and 15 for Samples Jan, Feb, Jul and Aug, respectively.

| | Jan vs Feb | | | | | Jul vs Aug | | | | |
|-----|------------|-----|-------------|----------|------------|------------|-----|-------------|----------|------------|
| | Edge-count | | p -values | | | Edge-count | | p -values | | |
| k | Jan | Feb | k th MST | k -MST | R_g -MST | Jul | Aug | k th MST | k -MST | R_g -MST |
| 1 | 15 | 20 | 0.034 | 0.034 | 0.034 | 24 | 18 | 0.003 | 0.003 | 0.003 |
| 2 | 15 | 18 | 0.112 | 0.007 | 0.008 | 12 | 14 | 0.533 | 0.272 | 0.038 |
| 3 | 14 | 19 | 0.105 | 0.002 | 0.003 | 18 | 16 | 0.516 | 0.138 | 0.050 |
| 4 | 14 | 16 | 0.540 | 0.003 | 0.002 | 21 | 19 | 0.031 | 0.008 | 0.019 |
| 5 | 13 | 8 | 0.109 | 0.090 | 0.005 | 14 | 16 | 0.916 | 0.020 | 0.014 |
| 6 | 15 | 14 | 0.902 | 0.108 | 0.009 | 10 | 17 | 0.259 | 0.082 | 0.018 |
| 7 | 15 | 10 | 0.558 | 0.279 | 0.019 | 10 | 24 | 0.009 | 0.026 | 0.017 |
| 8 | 19 | 14 | 0.468 | 0.231 | 0.029 | 13 | 14 | 0.723 | 0.072 | 0.020 |

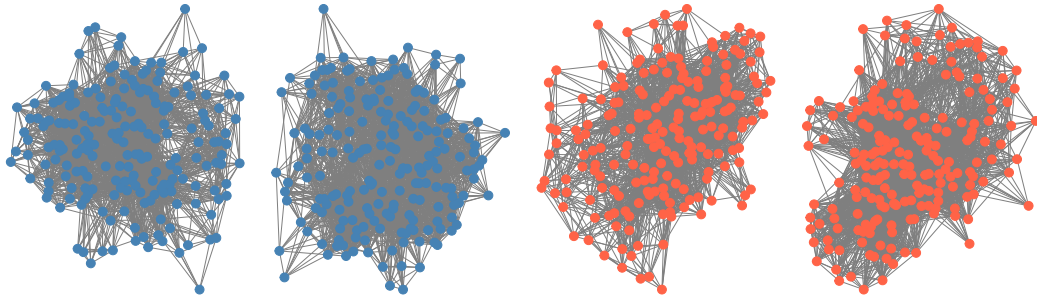


FIG 2. The brain networks of two male subjects (blue) and two female subjects.

TABLE 8
The p -values of the tests for the brain network data.

| Method | R_g -NN | R_o -MDP | GET | BD |
|-------------|---------------|---------------|---------------|-------|
| p -values | 0.004 (0.007) | 0.026 (0.025) | 0.005 (0.011) | 0.057 |

are then represented by 200×200 weighted adjacency matrices. For each subject, we use the average of their ten networks from different scans as their brain network representation, then we obtain fifteen networks for the male and female groups, respectively. For simplicity, we use the Frobenius norm as the distance measure.

The results are presented in Table 8. Since the sample size is small ($N = 30$), to check the validity of the asymptotic p -value approximation, we also show the p -values of GET and RISE from 1000 permutations, which are showed in the brackets. We notice that for RISE, the approximate p -values are very close to the p -values from permutations even in such a small sample size, which validates the effectiveness of the asymptotic approximation. All of these tests have small p -values. BD shows some evidence of difference with a p -value slightly larger than 0.05 but RISE can provide a more confident conclusion with smaller p -values. Besides, a heat map of the distance matrix of the 30 subjects is presented in Figure 3 where the first 15 subjects are male and the others female. We see an obvious difference between male and female subjects from the heat map, where the female subjects have smaller within-sample distances. These results support the conclusion from RISE that the male and female brain networks are different.

Appendix A: Proof of Theorem 2.1

Under the permutation null distribution, for $i \neq j \neq s \neq k$, we have

$$\begin{aligned} \mathbf{E}_P(g_i) &= m/N, & \mathbf{E}_P(g_i g_j) &= \frac{m(m-1)}{N(N-1)}, \\ \mathbf{E}_P(g_i g_j g_k) &= \frac{m(m-1)(m-2)}{N(N-1)(N-2)}, & \mathbf{E}_P(g_i g_j g_k g_s) &= \frac{m(m-1)(m-2)(m-3)}{N(N-1)(N-2)(N-3)}. \end{aligned}$$

Recall that \mathbf{R} is symmetric with zero diagonal elements. Then

$$\mathbf{E}_P(U_x) = \sum_{i=1}^N \sum_{j=1, j \neq i}^N R_{ij} \mathbf{E}_P(g_i g_j) = \frac{n(n-1)}{N(N-1)} \sum_{i=1}^N \sum_{j=1, j \neq i}^N R_{ij} = m(m-1)r_0,$$

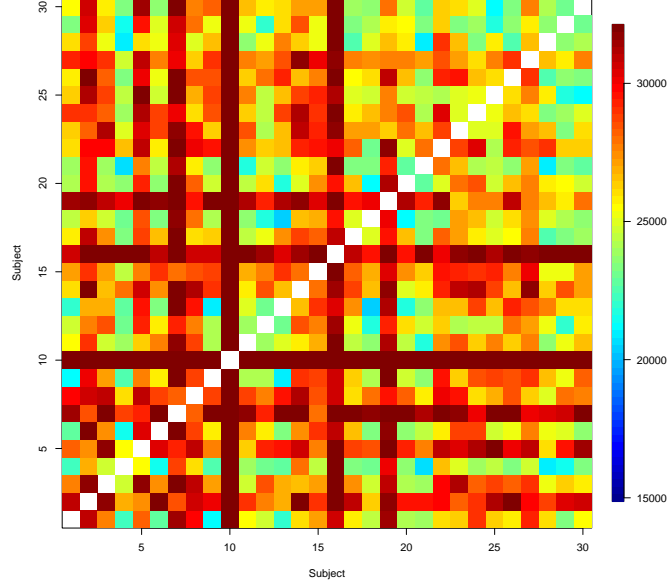


FIG 3. The heatmap of the distance matrix of the 30 subjects, where the first 15 subjects are male and the others female.

and similarly $\mathbf{E}_P(U_y) = n(n-1)r_0$. Then we have

$$\begin{aligned}
 \mathbf{E}_P(U_x^2) &= \sum_{i=1}^N \sum_{j=1}^N \sum_{s=1}^N \sum_{k=1}^N R_{ij} R_{sk} \mathbf{E}_P(g_i g_j g_s g_k) \\
 &= 2 \sum_{i=1}^N \sum_{j=1}^N R_{ij}^2 \mathbf{E}_P(g_i g_j) + 4 \sum_{i=1}^N \sum_{j=1}^N \sum_{k \neq i, j}^N R_{ij} R_{ik} \mathbf{E}_P(g_i g_j g_k) \\
 &\quad + \sum_{i=1}^N \sum_{j=1}^N \sum_{s \neq i, j}^N \sum_{k \neq i, j, s}^N R_{ij} R_{sk} \mathbf{E}_P(g_i g_j g_s g_k) \\
 &= \frac{m(m-1)n}{(N-2)(N-3)} \left\{ 2(n-1)r_d^2 + 4(m-2)(N-1)r_1^2 + \frac{N(N-1)(m-2)(m-3)}{n} r_0^2 \right\}.
 \end{aligned}$$

Combing with $\mathbf{Var}_P(U_x) = \mathbf{E}_P(U_x^2) - \mathbf{E}_P(U_x)^2$, we can obtain the variance of U_x under the permutation null distribution. Similarly for $\mathbf{Var}_P(U_y)$. Finally, we

have $\mathbf{Cov}_P(U_x, U_y) = \mathbf{E}_P(U_x U_y) - \mathbf{E}_P(U_x) \mathbf{E}_P(U_y)$, where

$$\begin{aligned}
 \mathbf{E}_P(U_x U_y) &= \sum_{i=1}^N \sum_{j=1}^N \sum_{s=1}^N \sum_{k=1}^N R_{ij} R_{sk} \mathbf{E}_P(g_i g_j (1 - g_s)(1 - g_k)) \\
 &= \sum_{i=1}^N \sum_{j=1}^N \sum_{s=1}^N \sum_{k=1}^N R_{ij} R_{sk} \left\{ \mathbf{E}_P(g_i g_j) - \mathbf{E}_P(g_i g_j g_s) - \mathbf{E}_P(g_i g_j g_k) + \mathbf{E}_P(g_i g_j g_s g_k) \right\} \\
 &= m(m-1)N(N-1)r_0^2 - 2 \frac{m(m-1)}{N(N-1)} \sum_{i=1}^N \sum_{j=1}^N R_{ij} (R_{i\cdot} + R_{j\cdot}) \\
 &\quad - 2 \frac{m(m-1)}{N(N-1)} \sum_{i=1}^N \sum_{j=1}^N R_{ij} (R_{i\cdot} + R_{j\cdot}) + \mathbf{Var}_P(U_x) \\
 &= m(m-1)N(N-1)r_0^2 - 4m(m-1)(N-1)r_1^2 \\
 &\quad - 2 \frac{m(m-1)(m-2)}{N(N-1)(N-2)} \{ N^2(N-1)^2 r_0^2 - 2N(N-1)^2 r_1^2 \} + \mathbf{Var}_P(U_x).
 \end{aligned}$$

We then finish the proof by plugging in the expression of $\mathbf{Var}_P(U_x)$.

Appendix B: Proof of Theorem 2.2

By Cauchy-Schwarz inequality, we have $r_1^2 \geq r_0^2$ and $r_d^2 \geq r_0^2$. When $m, n \geq 2$ and $r_1^2 \neq r_0^2$, we have $\mathbf{Var}_P(U_x) \neq 0$, $\mathbf{Var}_P(U_y) \neq 0$, and Σ is singular if and only if

$$\left| \frac{\mathbf{Cov}_P(U_x, U_y)}{\sqrt{\mathbf{Var}_P(U_x) \mathbf{Var}_P(U_y)}} \right| = 1.$$

We next solve the equation

$$\left(\mathbf{Cov}_P(U_x, U_y) \right)^2 - \mathbf{Var}_P(U_x) \mathbf{Var}_P(U_y) = 0,$$

which is equivalent to

$$\begin{aligned}
 0 &= 4(m-1)(n-1) \{ (r_d^2 - r_0^2)^2 - 4(N-1)(r_d^2 - r_0^2)(r_1^2 - r_0^2) + 4(N-1)^2 (r_1^2 - r_0^2)^2 \} \\
 &\quad - 4 \{ (m-1)(n-1)(r_d^2 - r_0^2)^2 + 4(m-2)(n-2)(N-1)^2 (r_1^2 - r_0^2)^2 \\
 &\quad + 2((m-1)(m-2) + (n-1)(n-2))(N-1)(r_d^2 - r_0^2)(r_1^2 - r_0^2) \} \\
 &= 8(N-1)(N-3)(r_1^2 - r_0^2) \left(2(N-1)(r_1^2 - r_0^2) - (N-2)(r_d^2 - r_0^2) \right).
 \end{aligned}$$

As a result, when $r_1^2 \neq r_0^2$ and $2(N-1)(r_1^2 - r_0^2) \neq (N-2)(r_d^2 - r_0^2)$, Σ is invertible, hence T_R is well-defined.

Appendix C: Proof of Theorem 2.3

Denote $\bar{\mathbf{U}} = (U_x - \mu_x, U_y - \mu_y)^\top$ and $\mathbf{A} = \begin{pmatrix} 1 & -1 \\ \frac{n-1}{N-2} & \frac{m-1}{N-2} \end{pmatrix}$. Since \mathbf{A} is invertible, we have

$$T_R = \bar{\mathbf{U}}^\top \boldsymbol{\Sigma}^{-1} \bar{\mathbf{U}} = \bar{\mathbf{U}}^\top \mathbf{A}^\top (\mathbf{A} \boldsymbol{\Sigma} \mathbf{A}^\top)^{-1} \mathbf{A} \bar{\mathbf{U}}.$$

It is easy to see that

$$\mathbf{A} \boldsymbol{\Sigma} \mathbf{A}^\top = \begin{pmatrix} (\sigma_{\text{diff}}^{\text{P}})^2 & 0 \\ 0 & (\sigma_w^{\text{P}})^2 \end{pmatrix}$$

and $\mathbf{A} \bar{\mathbf{U}} = (U_{\text{diff}} - \mathbf{E}_{\text{P}}(U_{\text{diff}}), U_w - \mathbf{E}_{\text{P}}(U_w))^\top$, thus finishing the proof.

Appendix D: Proof of Theorem 3.1

At first, we consider the bootstrap null distribution. The bootstrap null distribution places probability $1/2^N$ on each of the 2^N assignments of N observations to either of the two samples, i.e., each observation is assigned to sample \mathbf{X} with probability m/N and to sample \mathbf{Y} with probability n/N , independently from any other observations. Let \mathbf{E}_{B} , \mathbf{Var}_{B} , \mathbf{Cov}_{B} be expectation, variance and covariance under the bootstrap null distribution. It's not hard to see that the number of observations assigned to sample X may not be m . Let n_X be this number and $Z_X = (n_X - m)/\sigma^{\text{B}}$ where σ^{B} is the standard deviation of n_X under the bootstrap null distribution. Notice that the bootstrap null distribution becomes the permutation null distribution conditioning on $n_X = m$.

By applying Theorem 2.1 and making simplifications, we have that

$$\mu_w^{\text{P}} \equiv \mathbf{E}_{\text{P}}(U_w) = \frac{N(n-1)(m-1)}{N-2} r_0; \quad \mu_{\text{diff}}^{\text{P}} \equiv \mathbf{E}_{\text{P}}(U_{\text{diff}}) = (N-1)(m-n)r_0;$$

$$(\sigma_w^{\text{P}})^2 \equiv \mathbf{Var}_{\text{P}}(U_w) = \frac{2m(m-1)n(n-1)}{(N-2)^2(N-3)} \{(N-2)(r_d^2 - r_0^2) - 2(N-1)(r_1^2 - r_0^2)\}$$

and

$$(\sigma_{\text{diff}}^{\text{P}})^2 \equiv \mathbf{Var}_{\text{P}}(U_{\text{diff}}) = 4(N-1)mn(r_1^2 - r_0^2).$$

Since g_i 's are independent under the bootstrap null distribution, it's not hard to derive that

$$\begin{aligned} \mathbf{E}_{\text{B}}(U_x) &= \frac{m^2(N-1)}{N} r_0; & \mathbf{E}_{\text{B}}(U_y) &= \frac{n^2(N-1)}{N} r_0, \\ \mathbf{Var}_{\text{B}}(U_x) &= \frac{2m^2n^2(N-1)}{N^3} r_d^2 + \frac{4nm^3(N-1)^2}{N^3} r_1^2, \\ \mathbf{Var}_{\text{B}}(U_y) &= \frac{2m^2n^2(N-1)}{N^3} r_d^2 + \frac{4n^3m(N-1)^2}{N^3} r_1^2, \\ \mathbf{Cov}_{\text{B}}(U_x, U_y) &= \frac{2m^2n^2(N-1)}{N^3} r_d^2 - \frac{4n^2m^2(N-1)^2}{N^3} r_1^2, \end{aligned}$$

which implies that

$$\mu_w^B \equiv \mathbf{E}_B(U_w) = \frac{N-1}{N(N-2)}(Nmn - m^2 - n^2)r_0,$$

$$\mu_{\text{diff}}^B \equiv \mathbf{E}_B(U_{\text{diff}}) = (N-1)(m-n)r_0,$$

and

$$(\sigma_w^B)^2 \equiv \mathbf{Var}_B(U_w) = \frac{2(N-1)m^2n^2}{N^3}r_d^2 + \frac{4(N-1)^2nm(m-n)^2}{(N-2)^2N^3}r_1^2,$$

$$(\sigma_{\text{diff}}^B)^2 \equiv \mathbf{Var}_B(U_{\text{diff}}) = \frac{4(N-1)^2nm}{N}r_1^2, \quad \text{and} \quad (\sigma^B)^2 \equiv \mathbf{Var}_B(n_X) = \frac{mn}{N}.$$

By defining $Z_w^B \equiv (U_w - \mu_w^B)/\sigma_w^B$, $Z_{\text{diff}}^B \equiv (U_{\text{diff}} - \mu_{\text{diff}}^B)/\sigma_{\text{diff}}^B$, we express $(Z_w^P, Z_{\text{diff}}^P)$ in the following way:

$$\begin{aligned} \begin{bmatrix} Z_w^P \\ Z_{\text{diff}}^P \end{bmatrix} &= \begin{bmatrix} \sigma_w^B/\sigma_w^P & 0 \\ 0 & \sigma_{\text{diff}}^B/\sigma_{\text{diff}}^P \end{bmatrix} \begin{bmatrix} Z_w^B \\ Z_{\text{diff}}^B \end{bmatrix} + \begin{bmatrix} (\mu_w^B - \mu_w^P)/\sigma_w^P \\ (\mu_{\text{diff}}^B - \mu_{\text{diff}}^P)/\sigma_{\text{diff}}^P \end{bmatrix} \\ &= \begin{bmatrix} \sigma_w^B/\sigma_w^P & 0 \\ 0 & \sqrt{(N-1)/N} \end{bmatrix} \begin{bmatrix} Z_w^B \\ \sqrt{T}Z_{\text{diff}}^B \end{bmatrix} + \begin{bmatrix} (\mu_w^B - \mu_w^P)/\sigma_w^P \\ (\mu_{\text{diff}}^B - \mu_{\text{diff}}^P)/\sigma_{\text{diff}}^P \end{bmatrix}. \end{aligned} \quad (3)$$

where $T = r_1^2/(r_1^2 - r_0^2)$. Since the distribution of $(Z_w^P, Z_{\text{diff}}^P)$ under the permutation null distribution is equivalent to the distribution of $(Z_w^B, Z_{\text{diff}}^B) \mid Z_X = 0$ under the bootstrap null distribution, we only need show following two statements for proving Theorem 3.1:

- $(Z_w^B, \sqrt{T}(Z_{\text{diff}}^B - \sqrt{1-1/T}Z_X), Z_X)$ is asymptotically multivariate Gaussian distributed under the bootstrap null distribution and the covariance matrix of the limiting distribution is of full rank.
- $\sigma_w^B/\sigma_w^P \rightarrow c_w$; $(\mu_w^B - \mu_w^P)/\sigma_w^P \rightarrow 0$; $(\mu_{\text{diff}}^B - \mu_{\text{diff}}^P)/\sigma_{\text{diff}}^P \rightarrow 0$ where c_w is a positive constant.

From Statement (D), the asymptotic distribution of $(Z_w^B, \sqrt{T}Z_{\text{diff}}^B)$ conditioning on $Z_X = 0$ is a bivariate Gaussian distribution under the bootstrap null distribution, which further implies that the asymptotic distribution of $(Z_w^B, \sqrt{T}Z_{\text{diff}}^B)$ under the permutation null distribution is a bivariate Gaussian distribution. Then, with Statement (D) and equation (3), we have $(Z_w^P, Z_{\text{diff}}^P)$ is asymptotically bivariate Gaussian distributed under the permutation null distribution. Finally, plus the fact that $\mathbf{Var}_P(Z_w^P) = \mathbf{Var}_P(Z_{\text{diff}}^P) = 1$ and $\mathbf{Cov}_P(Z_w^P, Z_{\text{diff}}^P) = 0$, we have that $rS \xrightarrow{D} \chi_2^2$.

Since $r_d^2 \geq r_1^2 \geq r_0^2$ by Cauchy-Schwarz inequality, we have

$$(\sigma_w^P)^2 \asymp N^2(r_d^2 + r_0^2) \asymp N^2r_d^2; \quad (\sigma_w^B)^2 \asymp N^2r_d^2; \quad (\sigma_{\text{diff}}^P)^2 \asymp N^3(r_1^2 - r_0^2); \quad (\sigma_{\text{diff}}^B)^2 \asymp N^3r_1^2.$$

Since $\mu_{\text{diff}}^B - \mu_{\text{diff}}^P = 0$ and

$$\mu_w^B - \mu_w^P = \frac{mn}{N}r_0 \asymp Nr_0,$$

by Condition 3.6, we have

$$\frac{\mu_w^B - \mu_w^P}{\sigma_w^P} \asymp r_0/r_d \lesssim r_1/r_d \rightarrow 0.$$

We then finish the proof of Statement (D). The proof of Statement (D) is deferred to Supplement S1.

Acknowledgment

The authors were partly supported by NSF Grant DMS-1848579.

References

- ARROYO, J., ATHREYA, A., CAPE, J., CHEN, G., PRIEBE, C. E. and VOGELSTEIN, J. T. (2021). Inference for multiple heterogeneous networks with a common invariant subspace. *Journal of Machine Learning Research* **22** 1–49.
- BARALE, M. and SHIRKE, D. (2021). A test based on data depth for testing location-scale of the two multivariate populations. *Journal of Statistical Computation and Simulation* **91** 768–785.
- BICKEL, P. J. (1965). On Some Asymptotically Nonparametric Competitors of Hotelling’s T2 1. *The Annals of Mathematical Statistics* 160–173.
- BISWAS, M. and GHOSH, A. K. (2014). A nonparametric two-sample test applicable to high dimensional data. *Journal of Multivariate Analysis* **123** 160–171.
- BISWAS, M., MUKHOPADHYAY, M. and GHOSH, A. K. (2014). A distribution-free two-sample run test applicable to high-dimensional data. *Biometrika* **101** 913–926.
- BULLMORE, E. and SPORNS, O. (2012). The economy of brain network organization. *Nature Reviews Neuroscience* **13** 336–349.
- CHAUDHURI, P. (1996). On a geometric notion of quantiles for multivariate data. *Journal of the American Statistical Association* **91** 862–872.
- CHEN, H., CHEN, X. and SU, Y. (2018). A weighted edge-count two-sample test for multivariate and object data. *Journal of the American Statistical Association* **113** 1146–1155.
- CHEN, H. and FRIEDMAN, J. H. (2017). A new graph-based two-sample test for multivariate and object data. *Journal of the American statistical association* **112** 397–409.
- CHEN, H. and ZHANG, N. R. (2013). Graph-based tests for two-sample comparisons of categorical data. *Statistica Sinica* 1479–1503.
- CHU, L. and CHEN, H. (2018). Sequential change-point detection for high-dimensional and non-euclidean data. *arXiv preprint arXiv:1810.05973*.
- CHU, L. and CHEN, H. (2019). Asymptotic distribution-free change-point detection for multivariate and non-euclidean data. *The Annals of Statistics* **47** 382–414.

- CRADDOCK, R. C., JAMES, G. A., HOLTZHEIMER III, P. E., HU, X. P. and MAYBERG, H. S. (2012). A whole brain fMRI atlas generated via spatially constrained spectral clustering. *Human brain mapping* **33** 1914–1928.
- DEB, N. and SEN, B. (2021). Multivariate rank-based distribution-free non-parametric testing using measure transportation. *Journal of the American Statistical Association* 1–45.
- ERTOZ, L., STEINBACH, M. and KUMAR, V. (2002). A new shared nearest neighbor clustering algorithm and its applications. In *Workshop on clustering high dimensional data and its applications at 2nd SIAM international conference on data mining* **8**.
- FRIEDMAN, J. H. and RAFSKY, L. C. (1979). Multivariate generalizations of the Wald-Wolfowitz and Smirnov two-sample tests. *The Annals of Statistics* 697–717.
- GRETTON, A., BORGFWARDT, K., RASCH, M. J., SCHOLKOPF, B. and SMOLA, A. J. (2008). A kernel method for the two-sample problem. *arXiv preprint arXiv:0805.2368*.
- GRETTON, A., FUKUMIZU, K., HARCHAOU, Z. and SRIPERUMBUDUR, B. K. (2009). A Fast, Consistent Kernel Two-Sample Test. In *NIPS* **23** 673–681.
- GRETTON, A., SEJDINOVIC, D., STRATHMANN, H., BALAKRISHNAN, S., PONTIL, M., FUKUMIZU, K. and SRIPERUMBUDUR, B. K. (2012a). Optimal kernel choice for large-scale two-sample tests. In *Advances in neural information processing systems* 1205–1213. Citeseer.
- GRETTON, A., BORGFWARDT, K. M., RASCH, M. J., SCHÖLKOPF, B. and SMOLA, A. (2012b). A kernel two-sample test. *The Journal of Machine Learning Research* **13** 723–773.
- HALLIN, M. and PAINDAVEINE, D. (2004). Rank-based optimal tests of the adequacy of an elliptic VARMA model. *The Annals of Statistics* **32** 2642–2678.
- HALLIN, M. and PAINDAVEINE, D. (2006). Parametric and semiparametric inference for shape: the role of the scale functional. *Statistics & Decisions* **24** 327–350.
- HALLIN, M., DEL BARRIO, E., CUESTA-ALBERTOS, J. and MATRÁN, C. (2021). Distribution and quantile functions, ranks and signs in dimension d : A measure transportation approach. *The Annals of Statistics* **49** 1139–1165.
- HARCHAOU, Z., BACH, F. R. and MOULINES, E. (2007). Testing for Homogeneity with Kernel Fisher Discriminant Analysis. In *NIPS* 609–616. Citeseer.
- HEDIGER, S., MICHEL, L. and NÄF, J. (2019). On the use of random forest for two-sample testing. *arXiv preprint arXiv:1903.06287*.
- HENZE, N. (1988). A multivariate two-sample test based on the number of nearest neighbor type coincidences. *The Annals of Statistics* 772–783.
- INGALHALIKAR, M., SMITH, A., PARKER, D., SATTERTHWAITTE, T. D., ELLIOTT, M. A., RUPAREL, K., HAKONARSON, H., GUR, R. E., GUR, R. C. and VERMA, R. (2014). Sex differences in the structural connectome of the human brain. *Proceedings of the National Academy of Sciences* **111** 823–828.
- JIANG, R., ZUO, N., FORD, J. M., QI, S., ZHI, D., ZHUO, C., XU, Y., FU, Z., BUSTILLO, J., TURNER, J. A. et al. (2020). Task-induced brain connectivity

- promotes the detection of individual differences in brain-behavior relationships. *NeuroImage* **207** 116370.
- KIAR, G., BRIDGEFORD, E. W., RONCAL, W. R. G., CHANDRASHEKHAR, V., MHEMBERE, D., RYMAN, S., ZUO, X.-N., MARGULIES, D. S., CRADDOCK, R. C., PRIEBE, C. E. et al. (2018). A high-throughput pipeline identifies robust connectomes but troublesome variability. *bioRxiv* 188706.
- KIM, I., RAMDAS, A., SINGH, A. and WASSERMAN, L. (2021). Classification accuracy as a proxy for two-sample testing. *The Annals of Statistics* **49** 411–434.
- LI, J. (2018). Asymptotic normality of interpoint distances for high-dimensional data with applications to the two-sample problem. *Biometrika* **105** 529–546.
- LIU, Y.-W. and CHEN, H. (2020). A fast and efficient change-point detection framework for modern data. *arXiv preprint arXiv:2006.13450*.
- LIU, R. Y. and SINGH, K. (1993). A Quality Index Based on Data Depth and Multivariate Rank Tests. *Journal of the American Statistical Association* **88** 252–260.
- LOPEZ-PAZ, D. and OQUAB, M. (2016). Revisiting classifier two-sample tests. *arXiv preprint arXiv:1610.06545*.
- MARDEN, J. I. (1999). Multivariate rank tests. *STATISTICS TEXTBOOKS AND MONOGRAPHS* **159** 401–432.
- MENAFILOGLIO, A. and SECCHI, P. (2017). Statistical analysis of complex and spatially dependent data: a review of object oriented spatial statistics. *European journal of operational research* **258** 401–410.
- MUKHOPADHYAY, S. and WANG, K. (2020). A nonparametric approach to high-dimensional k-sample comparison problems. *Biometrika* **107** 555–572.
- OJA, H. (2010). *Multivariate nonparametric methods with R: an approach based on spatial signs and ranks*. Springer Science & Business Media.
- PAN, W., TIAN, Y., WANG, X. and ZHANG, H. (2018). Ball divergence: non-parametric two sample test. *Annals of statistics* **46** 1109.
- PAUL, B., DE, S. K. and GHOSH, A. K. (2021). HDLSSkST: Distribution-Free Exact High Dimensional Low Sample Size k-Sample Tests R package version 2.0.0.
- PURI, M. L. and SEN, P. K. (2013). On a class of multivariate multisample rank-order tests. In *Nonparametric Methods in Statistics and Related Topics* 659–682. De Gruyter.
- ROSENBAUM, P. R. (2005). An exact distribution-free test comparing two multivariate distributions based on adjacency. *Journal of the Royal Statistical Society: Series B (Statistical Methodology)* **67** 515–530.
- SARKAR, S., BISWAS, R. and GHOSH, A. K. (2020). On some graph-based two-sample tests for high dimension, low sample size data. *Machine Learning* **109** 279–306.
- SARKAR, S. and GHOSH, A. K. (2018). On some high-dimensional two-sample tests based on averages of inter-point distances. *Stat* **7** e187.
- SCHILLING, M. F. (1986). Multivariate two-sample tests based on nearest neighbors. *Journal of the American Statistical Association* **81** 799–806.
- SONG, H. and CHEN, H. (2020). Generalized Kernel Two-Sample Tests. *arXiv*

- preprint *arXiv:2011.06127*.
- SZÉKELY, G. J. and RIZZO, M. L. (2013). Energy statistics: A class of statistics based on distances. *Journal of statistical planning and inference* **143** 1249–1272.
- TIAN, Z., JIA, L., DONG, H., SU, F. and ZHANG, Z. (2016). Analysis of urban road traffic network based on complex network. *Procedia engineering* **137** 537–546.
- WILCOXON, F. (1945). Individual Comparisons by Ranking Methods. *Biometrics Bulletin* **1** 80–83.
- ZHANG, J. and CHEN, H. (2020). Graph-Based Two-Sample Tests for Data with Repeated Observations. *Statistica Sinica* DOI:10.5705/ss.202019.0116.
- ZHANG, Y. and CHEN, H. (2021). Graph-based multiple change-point detection. *arXiv preprint arXiv:2110.01170*.
- ZHOU, D. and CHEN, H. (2021). Supplement to "RISE: Rank In Similarity graph Edge-count two-sample test". *arXiv preprint arXiv:.*
- ZHU, Y. and CHEN, H. (2021). Limiting distributions of graph-based test statistics.
- ZUO, X.-N., ANDERSON, J. S., BELLEC, P., BIRN, R. M., BISWAL, B. B., BLAUTZIK, J., BREITNER, J. C., BUCKNER, R. L., CALHOUN, V. D., CASTELLANOS, F. X. et al. (2014). An open science resource for establishing reliability and reproducibility in functional connectomics. *Scientific data* **1** 1–13.